Human Molecular Genetics, 2013, Vol. 22, No. 15 **2992–3002**
doi:10.1093/hmg/ddt156
Advance Access published on April 4, 2013

Evolutionarily conserved long intergenic non-coding RNAs in the eye

Debarshi Mustafi[1], Brian M. Kevany[1], Xiaodong Bai[2], Tadao Maeda[3], Jonathan E. Sears[4], Ahmad M. Khalil[2,5] and Krzysztof Palczewski[1,*]

[1]Department of Pharmacology, [2]Center for RNA Molecular Biology, [3]Department of Ophthalmology and Visual Sciences and [4]Cole Eye Institute, Cleveland Clinic, Cleveland, OH 44106-4965, USA and [5]Department of Genetics and Genome Sciences, Case Western Reserve University, 10900 Euclid Ave, Cleveland, OH 44106-4965, USA

Received February 10, 2013; Accepted April 2, 2013

The discovery that the mammalian transcriptome encodes thousands of long intergenic non-coding (linc) RNA transcripts, together with recent evidence that lincRNAs can regulate protein-coding genes, has added a new level of complexity to cellular transcriptional/translational regulation. Indeed several reports now link mutations in lincRNAs to heritable human disorders. Here, we identified a subset of lincRNAs in terminally differentiated adult human retinal neurons based on their sequence conservation across species. RNA sequencing of eye tissue from several mammalian species with varied rod/cone photoreceptor content identified 18 lincRNAs that were highly conserved across these species. Sixteen of the 18 were conserved in human retinal tissue with 14 of these also conserved in the macular region. A subset of lincRNAs exhibited restricted tissue expression profiles in mice, with preferential expression in the retina. Mouse models with different populations of retinal cells as well as *in situ* hybridization provided evidence that these lincRNAs localized to specific retinal compartments, most notably to the photoreceptor neuronal layer. Computational genomic loci and promoter region analyses provided a basis for regulated expression of these conserved lincRNAs in retinal post-mitotic neurons. This combined approach identified several lincRNAs that could be critical for retinal and visual maintenance in adults.

INTRODUCTION

Genetic complexity in the ocular transcriptome of the adult retina (1) allows the encoding of a diverse set of proteins that support vision (2). However, work over the last few decades has revealed that non-coding RNAs can have a profound effect on the cellular transcriptional and translational landscape. Small non-coding RNAs such as microRNAs, first discovered in 1993 (3), were later reported in 2000 to have a universal post-transcriptional role across species (4) through translational regulation (5). Advances in next-generation sequencing along with closer examination of the human (6,7) and mouse (8) genomes revealed that the mammalian genome encodes thousands of long non-coding RNAs (9), including over 8000 long intergenic non-coding RNAs (lincRNAs) in the human genome (10). Transcribed from genomic loci flanked by two protein coding genes, lincRNAs are over 200 nucleotides long, undergo typical mammalian RNA processing involving 5′ capping, poly-adenylation and splicing, but have no protein-coding capability (11–13). LincRNAs reportedly regulate transcription of protein-coding genes by guiding and tethering chromatin modifying complexes to specific genomic loci in a *trans*-regulatory manner (13–15), but the precise mechanisms are still largely unknown as lincRNAs have also been shown to work in a *cis*-regulatory manner (16). Moreover, lincRNAs show a broad sub-cellular compartmentalization (17,18) implying that their functional contribution may occur at both the transcriptional and post-transcriptional levels. With increasing association of long non-coding RNAs with human disease (19–21) and recent evidence of lincRNAs related to Mendelian disorders and neurodevelopmental disabilities (22), there is a pressing need to understand the cellular roles of these molecules.

An importance of lincRNAs is supported by their highly tissue-specific expression (11) and location close to protein-coding genes associated with development and transcriptional

*To whom correspondence should be addressed. Tel: +1 2163684631; Fax: +1 2163681300; Email: kxp65@case.edu

regulation (16,23). Model organisms in which to study lincRNAs (24,25) together with emerging technologies (26) and collaboration with computational methods (27,28) will aid in delineating the cell-specific roles of these transcripts that are not only conserved at the sequence level, but also at the secondary structure level (29). But with no high-throughput methodology yet to assess lincRNA function, there exists a need to first identify and then filter lincRNAs in a cell-specific context. Identifying lincRNAs that display evolutionary sequence conservation across species in a particular tissue provides a first step in this endeavor.

The presence of lincRNAs in the adult retina would suggest a role in mediating vision in humans, a process dependent on strict transcriptional control of genes specific to terminally differentiated photoreceptor neurons. LincRNAs have been shown to influence both circadian control in the closely related pineal gland (30) and early stages of retinal development (31–36). The possible physiological roles of lincRNAs in post-mitotic neurons of the adult retina have yet to be investigated. Thus we carried out RNA-Sequencing (RNA-Seq) of eye tissue from a diverse set of adult mammalian species to document the conservation profile of lincRNAs relative to those of human retinal and macular tissue.

RESULTS

RNA-Seq identifies eye lincRNAs that exhibit sequence conservation in mammals and those that exhibit conservation in the human retina and macular region

We carried out RNA-Seq with eye tissue from a diverse set of mammalian species with varied retinal photoreceptor cellular compositions and distributions. We first analyzed three biological replicates of whole eye tissue from mice with three distinct genetic backgrounds: A/J, BALB/c and C57BL/6J (B6) (37). An RNA-Seq experiment of a retinal sample from B6 mice (38) was also included to guide transcript localization. Expression values were calculated as fragments per kilobase per million reads (FPKM) (39). With an expression cut-off of 1 FPKM, 103, 83 and 109 lincRNAs were detected in A/J, BALB/c and B6 mouse eyes, respectively, of which 48 were consistently expressed (Fig. 1A). These 48 lincRNAs were then investigated for conservation at the sequence level in eye tissue from three rodents with a range of photoreceptor populations and behavior patterning, namely *Rattus norvegeicus* (rat, nocturnal, ∼1% cones), *Arvicanthis niloticus* (Nile rat, diurnal, ∼33% cones) and *Ictidomys tridecemlineatus* (ground squirrel, diurnal, ∼97% cones), as well as the higher order mammal, *Macaca fasicularis* (monkey, diurnal, 5% cones, macula present). Data were analyzed by quality trimming the reads from each species and mapping them to the 48 consistently expressed mouse lincRNA sequences.

Using this methodology, we found 18 mouse lincRNAs to be conserved in the eye across all species examined (Fig. 1A and B). Many of these lincRNAs exhibited extremely high sequence conservation and further examination revealed that 16 of the 18 lincRNAs were also conserved in human retinal tissue subjected to RNA-Seq analysis (Fig. 1C). The conservation profile of lincRNAs in the eye and retina of the species (Supplementary Material, Tables S1 and S2) indicated that most localized to the retina, a perception further supported by examining the expression profile in B6 mice (Table 1). Although high-order mammals like monkeys and humans have only about 5% cone photoreceptors in their retina (40), a central region of the retina termed the macula, most specifically the fovea, is rich in cone photoreceptors and responsible for visual acuity and high-resolution vision (41). By specifically sequencing the macular region from four monkey biological replicates, we found that 14 of the 18 conserved lincRNAs across species were present (Fig. 2 and Supplementary Material, Table S3). Next, we probed these 18 transcripts in greater detail to determine their tissue-specific expression profiles in B6 mice.

Tissue and eye compartment expression of conserved lincRNAs

Expression profiles of the 18 conserved lincRNAs were investigated by isolating total RNA from a range of tissues in B6 mice and subjecting them to real-time polymerase chain reaction (RT-PCR) analysis. Eye, brain, heart, liver and lung tissue were chosen for their cellular complexity and diversity of biological function. Eye compartments including the lens/cornea, retina and retinal pigmented epithelium (RPE)/choroid were also examined separately. Specific primers used to amplify the product sequence of lincRNAs were subjected to Sanger sequencing which revealed 100% sequence overlap with the annotated sequence in Ensembl. Semi-quantitative RT-PCR (sqRT-PCR), which allowed us to establish transcript presence and absence at optimized cycles, showed the tissue enrichment profile of these lincRNAs (Supplementary Material, Table S4). These results were further evaluated with quantitative RT-PCR (qRT-PCR) of 6 selected lincRNAs that displayed broad organ and eye tissue distribution in expression profiles (Fig. 3). The sqRT-PCR and qRT-PCR results were in good agreement, with subtle differences attributable to the use of different custom primer sets for the experiments. A subset of lincRNAs evidenced expression restricted to just a few organs and specific eye compartments. *EyeLinc14*, for example, was more highly expressed in the eye relative to other organs examined and localized preferentially to the retina and RPE/choroid compartments. Targets such as *EyeLinc1* and *EyeLinc4* showed enrichment in just a few tissues, whereas others like *EyeLinc17* were expressed in most tissues assayed. Although many lincRNAs showed preferential expression in the retinal compartment of the eye, we sought to determine whether they were localized to specific retinal cell types.

Expression of some conserved lincRNAs is localized to specific retinal layers

To localize lincRNAs in the retina, we first used mouse models with different rod/cone ratios, a methodology previously employed to localize microRNAs to cellular components of the retina (42). Whereas in B6 mice all cellular components of the retina were preserved, in *Cone-DTA*$^{+/-}$ mice (*Cone-DTA)* cone photoreceptors were absent but rod photoreceptors were preserved (43), in *Nrl*$^{-/-}$ mice rod photoreceptors were absent and only cone-like photoreceptors were

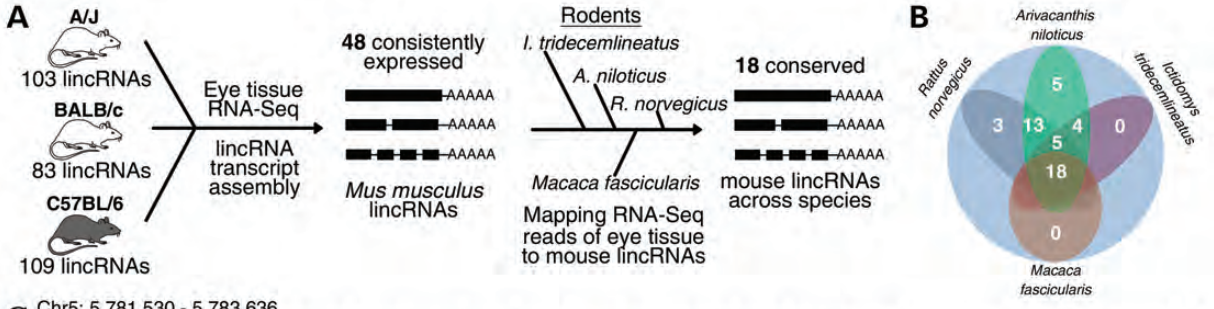

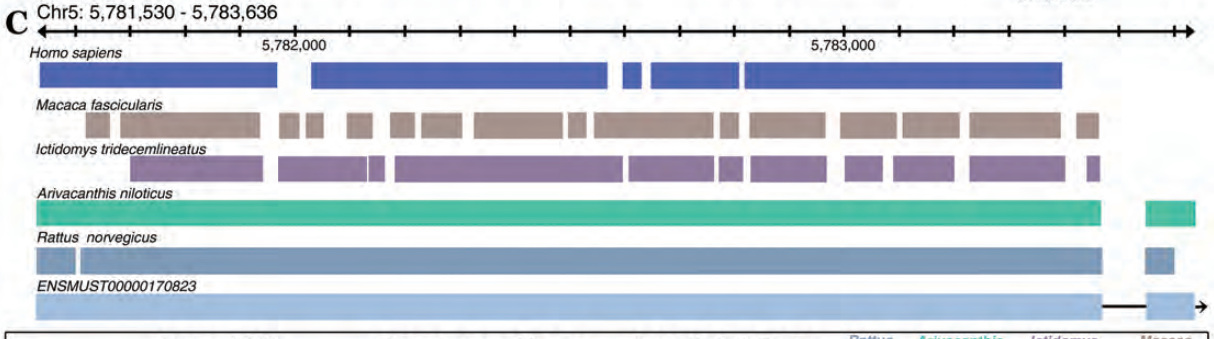

	Ensembl ID	Chromosomal Locus	Length (nt)	Exons	*Rattus norvegicus*	*Arivacanthis niloticus*	*Ictidomys tridecemlineatus*	*Macaca fascicularis*
EyeLinc1	*ENSMUST00000052354*	**Chr13**:83,878,485-83,880,912	2,427	1	1,578/0.65	1,781/0.73	920/0.38	851/0.35
EyeLinc2	*ENSMUST00000072769*	**Chr3**:121,958,875-121,996,467	1,802	2	926/0.51	960/0.53	720/0.40	644/0.36
EyeLinc3	*ENSMUST00000081739*	**Chr19**:10,273,678-10,276,872	3,194	1	1,458/0.46	1,610/0.50	507/0.16	441/0.14
EyeLinc4	*ENSMUST00000100847*	**Chr5**:115,552,930-115,560,277	683	2	426/0.62	451/0.66	305/0.45	336/0.49
EyeLinc5	*ENSMUST00000133910*	**Chr7**:100,327,492-100,328,179	687	1	652/0.95	686/1.00	556/0.81	512/0.75
EyeLinc6	*ENSMUST00000136359*	**Chr7**:149,761,433-149,764,048	2,286	5	1,980/0.87	2,023/0.88	251/0.11	298/0.13
EyeLinc7	*ENSMUST00000140208*	**ChrX**:148,924,203-148,926,403	2,200	1	1,308/0.59	1,438/0.65	1,065/0.48	1,050/0.48
EyeLinc8	*ENSMUST00000152262*	**ChrX**:148,867,019-148,869,219	2,200	1	1,337/0.61	1,394/0.63	1,052/0.48	1,062/0.48
EyeLinc9	*ENSMUST00000159347*	**Chr10**:28,600,726-28,642,201	618	2	288/0.47	337/0.55	158/0.26	126/0.20
EyeLinc10	*ENSMUST00000164531*	**Chr8**:4,088,148-4,089,166	711	2	512/0.72	642/0.90	279/0.39	243/0.34
EyeLinc11	*ENSMUST00000165677*	**Chr11**:117,281,950-117,283,031	669	2	443/0.66	480/0.72	379/0.57	290/0.43
EyeLinc12	*ENSMUST00000165869*	**Chr2**:120,358,639-120,365,582	3,328	2	2,128/0.64	1,663/0.50	361/0.11	365/0.11
EyeLinc13	*ENSMUST00000166167*	**Chr12**:84,961,159-84,962,124	850	2	697/0.82	812/0.96	652/0.77	621/0.73
EyeLinc14	*ENSMUST00000166576*	**Chr1**:182,732,698-182,739,614	2,550	2	731/0.29	971/0.38	629/0.25	586/0.23
EyeLinc15	*ENSMUST00000168221*	**Chr7**:46,843,887-46,847,049	2,927	2	1,973/0.67	1,984/0.68	910/0.31	733/0.25
EyeLinc16	*ENSMUST00000169263*	**Chr17**:25,931,838-26,101,729	1,902	2	830/0.44	979/0.51	310/0.16	298/0.16
EyeLinc17	*ENSMUST00000170823*	**Chr5**:5,781,529-5,783,636	2,026	2	1,968/0.97	2,023/1.00	1,490/0.74	1,412/0.70
EyeLinc18	*ENSMUST00000171491*	**Chr13**:98,521,066-98,530,920	1,073	3	581/0.54	585/0.55	489/0.46	544/0.51

Figure 1. RNA-Seq of eye tissue from rodents and higher order mammals reveals sequence conserved lincRNAs. (**A**) RNA-Seq of three biological replicates of whole eye tissues from A/J, BALB/c and C57BL/6J mice revealed 103, 83 and 109 lincRNAs (≥1 FPKM) in A/J, BALB/c and C57BL/6 mouse eyes, respectively, of which 48 were found consistently expressed across the three different mouse backgrounds. Of these 48 lincRNAs, 18 showed sequence conservation across different rodent species with variable retinal photoreceptor cell populations [*Rattus norvegeicus* (rat), nocturnal, ∼1% cones; *Arvicanthis niloticus* (Nile rat), diurnal, ∼33% cones; and *Ictidomys tridecemlineatus* (ground squirrel), diurnal, ∼97% cones] as well as a higher order mammal [*Macaca fasicularis* (monkey), diurnal, 5% cones, macula present]. (**B**) Diagram illustrating the conservation profile of the 48 mouse expressed lincRNAs with 18 conserved across all species and 5 conserved exclusively among rodents. Of the 18 conserved eye lincRNAs, 16 also were conserved in human retinal tissue. (**C**) Shown is an example of reads mapped to a mouse lincRNA. *ENSMUST00000170823* was chosen as it was the most highly expressed of the 18 conserved mouse lincRNAs. Portions of this mouse lincRNA transcript covered by reads from eye tissue of different species are presented. Interestingly, reads for the second exon were found in rodents closer to mouse (*Rattus norvegicus* and *Arivanathis niloticus*), but not detected in *Ictidomys tridecmelineatus*, *Macaca fasicularis* or *Homo sapiens* samples. A table of all 18 conserved lincRNAs is shown below. For each species, the lincRNA transcript covered by reads was calculated and presented as the total number of nucleotides (nt) in the specified lincRNA transcript and portions of the entire length of the transcript covered by the reads. For example, of the 2247 bases of EyeLinc1 in *Rattus norvegicus*, there were reads of 1578 bases encompassing 0.65 of the entire transcript. The 16 lincRNAs listed in blue also exhibited sequence conservation in the human retina.

present (44), and in aged (7-month-old) *P23H* mice there were no photoreceptors detected but other layers of the neural retina were retained (45) (Fig. 4A). Total RNA extracted from eyes of these mice was then subjected to RT-PCR analysis for lincRNA expression levels. The sqRT-PCR (Supplementary Material, Table S5) results, further quantified by qRT-PCR of selected targets (Fig. 4B), suggested possible localization of the lincRNAs to specific retinal layers. Enriched expression of *EyeLinc2* and *EyeLinc7/8* in B6 and *Cone-DTA* mice together with greatly reduced expression in $Nrl^{-/-}$ mice and some residual expression in *P23H* mice suggested their possible localization to the photoreceptor layer, as this pattern resembled the profile of *Abca4* expression, with a gene product that resides in photoreceptor discs (46). *EyeLinc14* displayed higher expression in B6 and *Cone-DTA* mice compared with reduced expression in $Nrl^{-/-}$ and *P23H* mice.

Table 1. Transcript abundance (FPKM) in the eye and retina of B6 mice for the 18 lincRNAs conserved across species and protein coding photoreceptor and RPE genes *Abca4*, *Opn1mw* and *Rpe65*

	B6 eye	B6 retina
EyeLinc1	4.31	5.16
EyeLinc2	35.22	38.05
EyeLinc3	2.58	3.25
EyeLinc4	85.89	39.22
EyeLinc5	108.25	73.18
EyeLinc6	6.62	0.14
EyeLinc7	4.94	5.64
EyeLinc8	4.94	5.64
EyeLinc9	1.73	1.18
EyeLinc10	4.74	0.00
EyeLinc11	16.07	3.29
EyeLinc12	7.72	11.28
EyeLinc13	11.93	4.33
EyeLinc14	7.51	10.12
EyeLinc15	4.46	4.86
EyeLinc16	9.15	0.00
EyeLinc17	199.39	193.64
EyeLinc18	30.57	21.36
Abca4	59.00	140.14
Opn1sw	117.79	187.21
Rpe65	67.21	17.63

Similarities in the abundance of many of these lincRNAs between whole eye and retina indicate their probable localization.

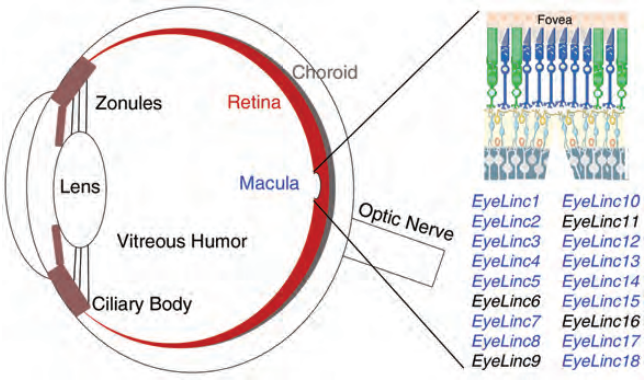

Figure 2. LincRNAs displaying conservation in the macular region of the retina highlight their potential role in higher order visual processing. RNA-Seq analysis of 4 biological replicates of monkey macula tissue revealed that of the 18 conserved lincRNAs identified across all species, 14 of them (shown in blue) were conserved in the macular region.

Markedly reduced *Eyelinc14* expression in the latter two mouse models suggests that this lincRNA primarily localizes to both rod photoreceptors and other retinal cellular compartments such as the RPE, in agreement with the results shown in Figure 3.

To further investigate the lincRNA localization inferred from these mouse models, we carried out *in situ* hybridization of *EyeLinc2*, *EyeLinc7/8*, *EyeLinc14* and *EyeLinc17* in the mouse retina by establishing a new methodology in frozen mouse retinal sections that allowed sensitive single-molecule RNA detection with almost no background. Mouse *ubiquitin c* (*Ubc*) was used as a positive control, whereas *E. coli dihydrodipicolinate reductase* (*dapB*) was used as a negative control for these hybridization assays. All lincRNAs were detected above the negative control background and signals in the photoreceptor regions were localized to the inner photoreceptor cell segments (Fig. 4C). *EyeLinc14* was notably detected in both the photoreceptor inner segment and RPE layers, consistent with localization findings from previous PCR experiments shown in Figures 3 and 4B. Therefore, the localization of these lincRNAs to specific retinal compartments, especially their enrichment in the neuronal photoreceptor cell layer, suggests that lincRNAs could have an important role in supporting vision. Next, we carried out a computational analysis of the conserved lincRNA loci and analyzed their promoter regions for binding motifs of transcription factors.

Genetic loci and *in silico* analyses of promoter motifs highlight possible roles of lincRNAs in adult retinal homeostasis

EyeLinc2 not only lies adjacent to the photoreceptor gene *Abca4* in the mouse genome (Fig. 5A), but its expression pattern is suggestive of photoreceptor localization (Fig. 4B and C). Support for possible involvement of these lincRNAs in retinal homoeostasis was investigated by analyzing transcription factor-binding motifs present in the 5 kb promoter regions of all 18 conserved lincRNAs with the JASPAR CORE 2009 database. Promoter motifs for binding of 17 unique transcription factors were found in these 18 lincRNAs, of which 13 mapped to multiple transcripts (Supplementary Material, Table S6). Analysis of transcription factor-binding site motifs in the context of retinal cell biology suggested that these conserved lincRNAs could play physiological roles in retinal homeostasis. Investigation of the promoter region of *EyeLinc2* revealed binding sites for genes such as *HMG-I(Y)* ($P = 2.13 \times 10^{-6}$) and *Sp1* ($P = 6.58 \times 10^{-6}$) implicated in regulating photoreceptor gene expression (47,48) (Fig. 5A). Consistent with the retina (49) and long non-coding RNAs (30) displaying circadian rhythmicity, *EyeLinc2* displayed statistically significant temporal changes in its expression level during the day (Fig. 5A). The promoter regions of *EyeLinc7/8*, *EyeLinc14* and *EyeLinc17* are also highlighted (Fig. 5B) to illustrate binding motifs of other genes implicated in photoreceptor and adult retinal homeostasis such as *Pax4* (50) and *CTCF* (51,52) of which *CTCF* has been shown to regulate gene expression in concert with a non-coding RNA (53).

DISCUSSION

The hypothesis that long non-coding RNAs in intergenic regions of the human genome possess functional roles (54) in normal homeostasis of post-mitotic retinal neurons and that their disregulation can lead to human diseases (55) necessitates a detailed understanding of these transcripts. The shear number of the lincRNA population makes it difficult to elucidate their physiological contribution to a specific tissue, but a first step would be to identify those that are conserved across species in specific tissues. Using high-throughput RNA-Seq methodology, we identified 18 lincRNAs in the adult eye that showed sequence conservation across a diverse range of species, from nocturnal rod-dominant rodents such as mouse

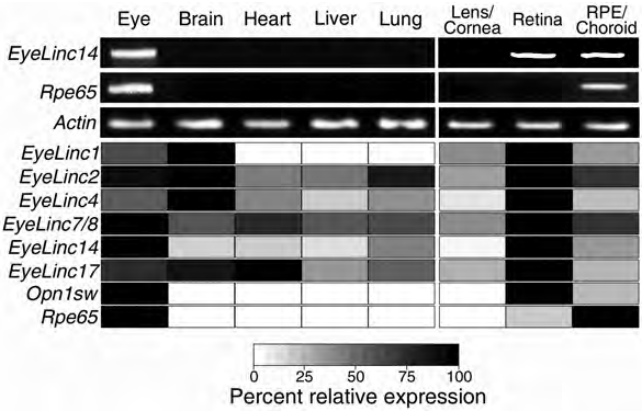

Figure 3. LincRNAs display spatially restricted expression in adult B6 mouse organs and eye compartments. Semi-quantitative RT-PCR of all 18 conserved lincRNAs revealed tissue-specific expression, such as for *EyeLinc14*, which not only revealed enriched expression in the eye relative to other organs but was also more preferentially expressed in the retina and RPE/choroid. *Rpe65*, a gene expressed only in the RPE of the eye, is shown as a positive control, whereas *Actin* was used for a loading control. The heat map below shows qRT-PCR results for six selected lincRNAs and two positive controls (*Opn1sw* and *Rpe65*) in the different organs and eye compartments. *EyeLinc7* and *EyeLinc8*, identical in sequence from a duplication in the X chromosome, are listed as *EyeLinc7/8*. Areas are shaded according to the relative levels of transcription normalized to the tissue/compartment with the highest expression levels ranging from 0% (white, undetectable) to 100% (black, highest).

and rat, to cone-dominant diurnal rodents such as the Nile rat and ground squirrel, to the diurnal monkey which like humans, possesses a cone-rich macula and rod-rich peripheral retina. Moreover, 16 of these 18 lincRNAs were found conserved in the human retina with 14 of these 18 also conserved in the macular region of the retina. A subset of these lincRNAs exhibited expression restricted to certain tissues in the mouse. Mouse models with different retinal cell populations along with *in situ* hybridization were used to further localize these lincRNAs to specific cellular layers of the retina, most notably the neuronal photoreceptor layer. Complementation of the cellular work with computational analysis of transcription factor-binding site motifs of the 18 conserved lincRNAs was a critical step in revealing a contribution of these transcripts in retinal homeostasis. In the absence of proper retinal cell lines to accurately identify *in vivo* functionality of these transcripts, more detailed roles of individual lincRNAs should become evident from cellular phenotypes that result when the cohort of conserved lincRNA loci identified in this work are disrupted.

Evolutionary pressure drives rapid sequence alterations of lincRNAs even in closely related species (56) highlighting the functional importance of those transcripts that remain conserved across species (57). Identification of 18 conserved lincRNAs from the initial 3133 mouse lincRNAs agrees with past studies that only a small minority of lincRNAs in the mouse or human have transcribed orthologous sequences in the other species (11). Identification of conserved lincRNAs that persisted despite evolutionary pressure across the diverse adult species studied (Figs 1 and 2) implies that these transcripts could potentially coordinate essential transcriptional/translational roles in adults when all retinal components are fully developed. These conserved lincRNAs exhibited a 100-fold expression range in the B6 mouse eye and retina (Table 1), but even those marginally expressed lincRNAs could fulfill vital roles such as basal regulation of protein-coding genes (55).

Closer examination of these 18 lincRNAs in B6 mice revealed that whereas some transcripts such as *EyeLinc17* displayed ubiquitous expression in the several tissues assayed, others such as *EyeLinc14* displayed tissue-restricted expression. *EyeLinc14* not only displayed enriched expression in the eye relative to other organs assayed, but it also was preferentially located in the retina and RPE, two layers that intimately collaborate to drive vision. Expression in tissues outside the eye does not preclude those lincRNAs from having retina-specific roles. Indeed *Tug1*, a non-coding RNA shown to be important at early stages of photoreceptor development, displayed robust expression in tissues besides the eye (35). As to the retina, we first localized lincRNAs in mouse models with subtle differences in retinal architecture (Fig. 4A and B) that had been previously used to localize non-coding RNAs (42). *In situ* hybridization (Fig. 4C) was then used to localize certain lincRNAs to specific retinal compartments, most notably to the neuronal photoreceptor and RPE layers of the retina.

Complementation of the above cellular studies with computational analysis of the genomic loci and promoter regions of all conserved lincRNAs provided insights into their possible roles in retinal homeostasis (Fig. 5). *EyeLinc2* exhibited an enrichment and localization pattern suggestive of photoreceptor expression (Fig. 4B and C) and lies adjacent in the mouse genome to *Abca4* (Fig. 5A), an essential photoreceptor protein product for removal of toxic retinoid metabolites (58) that can cause severe retinopathies if mutated (59,60). Promoter analysis of *EyeLinc2* revealed that it possesses binding sites for *HMG-I(Y)*, which is rarely expressed in terminally differentiated cells, but it is enriched in photoreceptor cells and thought to accommodate the daily induction of phototransduction and visual cycle genes such as *Abca4* (48). Consistent with the diurnal nature of gene expression in the retina, HMG-box proteins evidence diurnal rhythms in photoreceptors (61), and *EyeLinc2* also displayed temporal changes in expression levels with a 1.7-fold elevation in the afternoon when compared with the morning (Fig. 5A). Temporal cycling of lincRNAs in the eye adds another dimension to their possible regulatory function (30). Examination of other lincRNAs revealed promoter regions for genes such as *Pax4* and *CTCF*. Unlike the master regulator homeobox-containing *Pax6* involved in eye morphogenesis (62), both *Pax4* (50) and *CTCF* (52) are developmentally segregated and display highest expression in photoreceptor cells of the adult retina. *Pax4* is thought to regulate gene expression in the mature retina (50) and can activate expression of rod-derived cone viability factor (63), a novel trophic factor that can protect cone photoreceptors from degenerating (64) and thus serve as alternative therapy for patients with retinitis pigmentosa (65). Meanwhile, recent evidence revealed that *CTCF* regulates the ataxin-7 gene through interactions with a non-coding RNA (53). Dysfunction in ataxin-7 leads to spinocerebellar ataxia type 7 and has been shown to produce photoreceptor dysfunction (66,67) and retinal degeneration (68). Moreover, overlapping disease pathways recently demonstrated for this neurodegenerative disorder and age-related

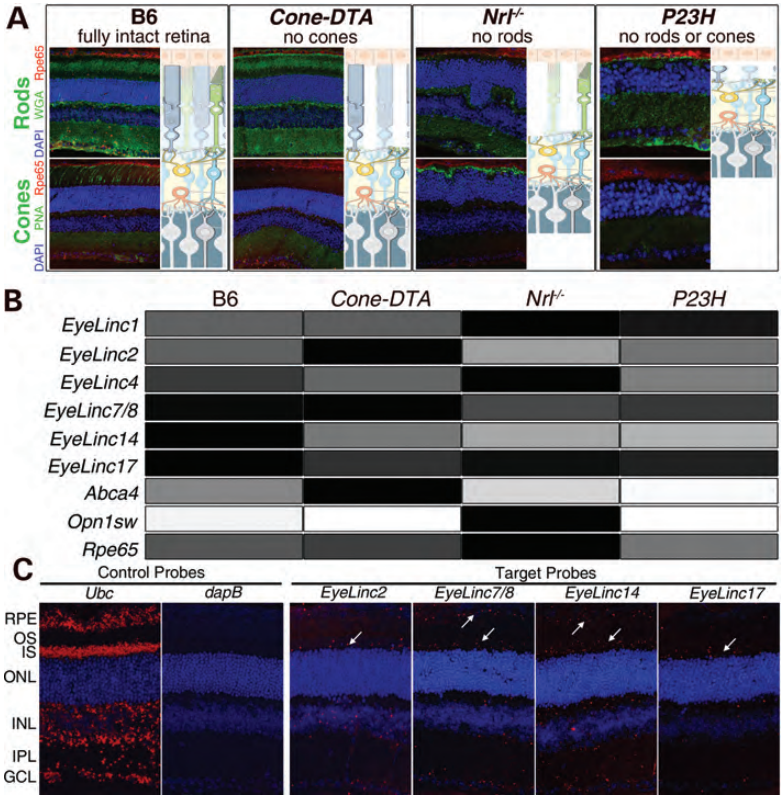

Figure 4. Enrichment profiles in mouse models with varying photoreceptor populations and *in situ* hybridization reveal cellular localization of lincRNAs to specific retinal layers. Mouse models that differ in their retinal architecture were analyzed: (**A**) B6 mice exhibited a fully intact retina with staining of the RPE layer as well as rod and cone photoreceptors; *Cone-DTA* mice featured an intact retina with RPE and rod photoreceptor staining but no cone photoreceptor signals; $Nrl^{-/-}$ mice displayed staining of the RPE layer and cone photoreceptors but no rod photoreceptor signals; and aged *P23H* mice had a degenerated photoreceptor layer with severely attenuated residual rod and cone photoreceptor staining, whereas the RPE layer stained with an antibody against RPE65 was normal. Rods and cones were stained with the lectins, WGA and PNA, respectively. Nuclei were stained with DAPI. (**B**) Expression of selected lincRNAs assessed by qRT-PCR of eye tissue from these mouse models is shown as a heatmap shaded as in Figure 3. In addition to the six selected lincRNAs, three controls were run: *Abca4*, a gene product that resides in photoreceptor discs; *Opn1sw*, a cone photoreceptor marker; and *Rpe65*, a RPE cell marker. (**C**) Mouse *Ubc* and *E. coli dapB* were used as positive and negative controls, respectively, to carry out *in situ* hybridizations in mouse retinas. Nuclei were stained with DAPI. LincRNA probes exhibiting the most prominent signals in the photoreceptor regions were localized to inner segments (denoted by downward-pointing white arrows), with expression in some cases in the RPE layer (denoted by upward-pointing white arrows). Layers are labeled as RPE, retinal pigmented epithelium; OS, outer segment; IS, inner segment; ONL, outer nuclear layer; INL, inner nuclear layer; IPL, inner plexiform layer; GCL, ganglion cell layer.

macular degeneration (69) highlight that these lincRNAs can have homeostatic roles beyond the retina. Thus, our *in silico* analysis highlights potential involvements of these conserved lincRNAs, not only in the maintenance of adult retinal homeostasis, but also in interacting with key retinal transcription factors for potential therapy of human retinopathies.

The dynamic process of vision requires a high level of expression to maintain photoreceptor specific genes that carry out phototransduction and the visual cycle (2), a process potentially affected by lincRNAs (70). This study suggests how in adult terminally differentiated post-mitotic retinal photoreceptor cells, lincRNAs could play a critical role in physiology of these cells. As understanding of the transcriptional landscape in human cells improves (71), accurate assembly of lincRNAs in tissue-specific contexts through high-throughput sequencing approaches constitutes the first step to identifying those transcripts that are likely to be important and warrant more detailed investigation. With increasing evidence that long non-coding RNAs such as lincRNAs are associated with common diseases (72) and constitute potential drivers of cancerous states (73), it is imperative to investigate those that could influence such pathology. That these transcripts can be targeted in mouse models of human disease to correct pathological states (74) also provides hope that their improved understanding will shape future therapeutics.

MATERIALS AND METHODS

Eye and retina tissue collection

A/J, BALB/c, C57BL/6 (B6) and *Cone-DTA* strains of mice, all 4 weeks of age, were obtained from The Jackson Laboratory (Bar Harbor, ME, USA). *P23H* knock-in mice generated in our laboratory (45) were 7 months of age. Four-week-old *Nrl*-deficient mice with a B6 background were obtained from Dr Anand Swaroop (University of Michigan, Ann Arbor, MI, USA). Long-Evans rats (*Rattus norvegeicus*), 4 weeks of age, were purchased from Harlan Laboratories (Madison, WI, USA). Nile rats (*Arvicanthis niloticus*), 6

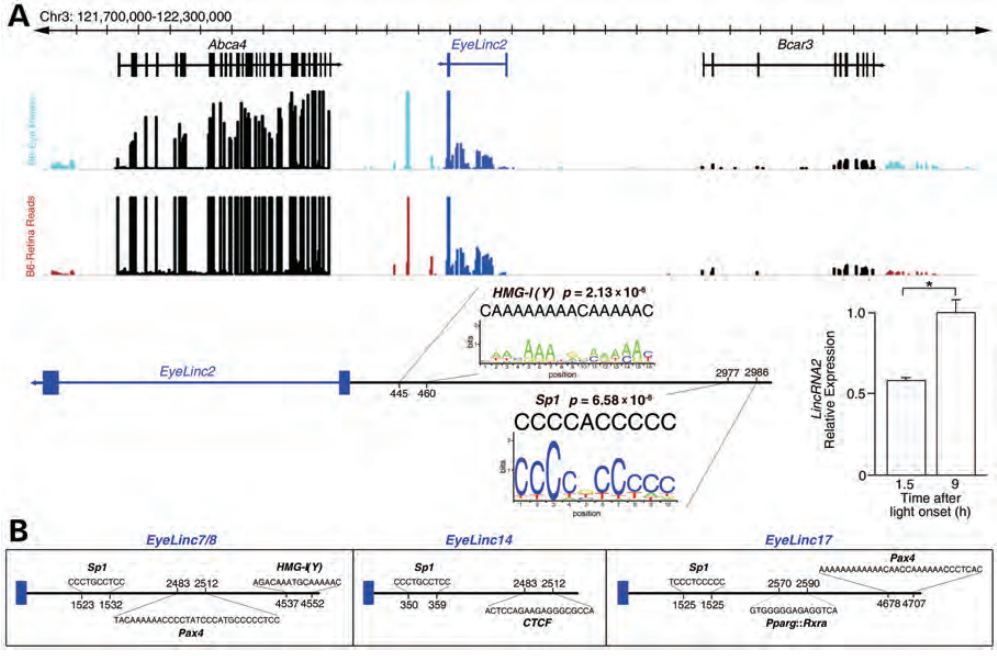

Figure 5. Location in the mouse genome and promoter analysis highlights possible roles for lincRNAs in retinal homeostasis. (**A**) Chromosomal location of the *Abca4* and *Bcar3* genes and the intergenic *EyeLinc2*. Plots show the RNA-Seq read coverage of these transcripts in the whole eye and retina of B6 mice. The promoter regions relative to the transcribed region of *EyeLinc2* highlight conservation of each promoter motif and the corresponding sequence found along with the *P* value for each motif occurrence are displayed. *EyeLinc2* also exhibited temporal changes in expression with a 1.7-fold increased expression at 9 h compared with 1.5 h after lights were turned on ($P < 0.01$). (**B**) Promoter regions relative to transcribed regions highlight different transcription factor-binding motifs found in *EyeLinc7/8*, *EyeLinc14* and *EyeLinc17*.

weeks of age, were obtained from the laboratory of Dr Laura Smale (Michigan State University, Lansing, MI, USA). Wild caught adult ground squirrels (*Ictidomys tridecemlineatus*) were purchased from TLS Research (Bloomingdale, IL, USA). Mice, rats and ground squirrels were housed in the Case Western Reserve University (CWRU) animal facility where they were maintained on a standard chow diet in a 12 h light (∼10 lux)/12 h dark cycle. After euthanizing animals, eye and retina tissue were collected and placed in a solution of RNAlater (Qiagen, Valencia, CA, USA) for processing. Enucleated macaque (*Macaca fascicularis*) eyes in RNAlater from 4-year-old animals were obtained from Ricerca Biosciences (Painesville, OH, USA). Clinical evaluations of the human patient from whom retinal tissue was obtained were carried out at the Cleveland Clinic Cole Eye Institute (Cleveland, OH, USA). This research conformed to the tenets of the Declaration of Helsinki. The retina was carefully dissected out of an untreated eye from a patient requiring enucleation for a large ocular melanoma and immediately placed in RNALater; the retinal sample was obtained from a hemiretina free of tumor. This eye had no abnormal neovascularization of the iris or retina and lacked signs of inflammation.

Library preparation and Illumina RNA-Seq runs

Eye and retina tissue libraries were prepared as previously described (37,38). Each mouse library was run on the Illumina Genome Analyzer IIx (Illumina, San Diego, CA, USA) in the CWRU Genomics core facility using 36–79 bp single-end read lengths. The processed and raw fastq files were previously deposited in GEO (accession numbers GSE38359 and GSE29752). Prepared libraries of Long-Evans rat eye and retinal tissues and human retinal tissue were sequenced by single-end sequencing, whereas prepared libraries of Nile rat, ground squirrel and macaque eye and retina tissue were sequenced by paired-end sequencing technology with the Illumina Genome Analyzer IIx or HiScan SQ.

Expression of lincRNAs in mouse eye and retina

Sequence information of 3133 identified lincRNAs in the mouse was extracted from Ensembl release 67. The Illumina reads from each mouse replicated tissue sample were processed separately. A quality trimming step was performed to remove bases from both ends with quality scores equivalent to a Phred quality score lower than 20. Only reads with 20 bases or longer after quality trimming were retained for further analysis. Trimmed reads were aligned to the mouse genome release mm9 with TopHat v2.0.0 (75). Aligned reads were assembled under the guidance of mm9 RefSeq and Ensembl lincRNA transcripts. Expression values were calculated as fragments per kilobase of exon model per million mapped reads (FPKM) for each lincRNA.

Conservation of mouse lincRNAs in different species

Reads from eye and retinal tissue samples of the different species were trimmed of bases with Phred quality scores of lower than 20. Reads that were less than 20 bases after such trimming were discarded. Reads from technical replicate

lanes were combined before being mapped to the mouse lincRNA sequences with TopHat v2.0.0 (75) and the resulting alignment files were processed with custom Perl scripts. Alignments with large (>3 base) insertions or deletions or reads of low complexity (≥80% of the reads were dinucleotide repeats or contained 8 or more consecutive A- or T-bases) were removed before the number of original reads and unique reads aligned to mouse lincRNA transcripts were counted. Portions of mouse lincRNA transcripts covered by reads were calculated and presented as bases and portions of the entire length of the transcript. If a mouse lincRNA transcript was aligned to five or fewer unique reads from a sample or the read coverage of the lincRNA transcript was <10%, then the mouse lincRNA transcript was not considered to be conserved in that species sample.

Promoter analysis

Each 5 kb promoter sequence of the 18 conserved lincRNA transcripts was searched with FIMO (76) for motifs in the JASPAR CORE 2009 database (http://jaspar.genereg.net/) and only those that returned statistically significant *P*-values with a position-specific scoring matrix for each of the motifs in the promoter sequences were considered. The 5 kb promoter sequences of all annotated genes in mouse genome release mm9 were also searched for motifs in the JASPAR CORE 2009 database. Motif enrichment in the promoter regions of the 18 conserved lincRNAs compared with genome-wide promoter regions was assessed with the Fisher's exact test using a Bonferroni correction.

Immunohistochemistry

All procedures used were reported previously (77). Cross-sections of mouse eyecups were incubated with primary antibodies, namely anti-mouse RPE65, biotinylated peanut agglutinin (PNA) and wheat germ agglutinin (WGA). Signals were detected with Cy3- or Alexa488-conjugated secondary antibody. Nuclear staining was achieved with 4′,6-diamidino-2-phenylindole (DAPI). Sections were analyzed with a Leica TCS SP5 II confocal microscope (Leica, Wetzlar, Germany).

In situ hybridization

The QuantiGene ViewRNA (Affymetrix, Santa Clara, CA, USA) *in situ* hybridization protocol was optimized by Affymetrix for use with fresh frozen mouse eye tissue samples. The protease concentration was increased 4-fold from a 1:100 to a 1:25 dilution and the incubation time was set at 40 min from the standard protocol for optimized signal strength and tissue morphology preservation. Slides were incubated with either *EyeLinc2* (VB1-13468), *EyeLinc7/8* (VB1-13469), *EyeLinc14* (VB1-13470) or *EyeLinc17* (VB1-13471) Fast Red probe sets for detection with a Leica TCS SP5 II confocal microscope. Slides incubated with the mouse *Ubc* (VB1-10202) Fast Red probe set were used for a positive control, whereas slides incubated with the *E. coli dapB* (VF1-10272) Fast Red probe set, employed as a negative control, were used to establish a background signal for the assay. Rat kidney FFPE tissue slides as a positive (Rat *Ubc* probe set, VC1-10190) and a negative (*E. coli dapB* probe set, VF1-10272) control were also analyzed to demonstrate that the assay reagents and the assay protocol were properly followed.

Semi-quantitative real-time PCR

Total RNA from B6 mouse tissues, including the eye, brain, heart, liver, lung, cornea/lens, retina and RPE/choroid, was purified by using the RNeasy Mini Kit with On-column DNase treatment (Qiagen). Each of the 18 lincRNAs identified to be conserved in all species was probed with the Qiagen One-step RT-PCR Kit. Twenty five nanograms of total RNA was used in each 12.5 μl reaction as per the manufacturer's instructions. Primers used to probe lincRNAs were custom designed to span introns whenever possible to rule out genomic DNA contamination. *Actin* primers were designed for loading controls and primers against *Nrl* (retina) and *Rpe65* (RPE) were employed to confirm the fidelity of tissue dissections.

Quantitative real-time PCR

One microgram of isolated eye, brain, heart, liver and lung tissue RNA from two pooled B6 mice, 1 μg of cornea/lens, retina and RPE/choroid tissue RNA from two pooled B6 mice and 1 μg of eye tissue RNA from B6, *Cone-DTA, Nrl*$^{-/-}$, and *P23H* mice were converted to cDNA with the High Capacity RNA-to-cDNA kit (Applied Biosystems, Foster City, CA, USA). RT-PCR was done with TaqMan chemistry and Assays on Demand probes (Applied Biosystems) for mouse *Abca4* (Mm00492035_m1), *Opn1sw* (Mm00432058_m1), *Rpe65* (Mm00504133_m1) and ABI custom designed primers for *EyeLinc1* (AIX00TR), *EyeLinc2* (AIW2NJ), *EyeLinc4* (AIS074V), *EyeLinc7/8* (AIVI4HB), *EyeLinc14* (AIT96A3) and *EyeLinc17* (AIRR9YN). The 18S rRNA (4319413E) probe set (Applied Biosystems) was used as the endogenous control. All real-time experiments were done in triplicate with the ABI Step-One Plus qRT-PCR machine (Applied Biosystems). Fold changes were calculated based on differences in threshold cycles (C_t) after normalization to 18S rRNA. Percent relative expression is presented as a percent of the maximal normalized expression observed in the different samples.

Statistical analysis

Experimental results were analyzed by an independent two-sample *t*-test. A *P*-value of 0.05 or less was considered statistically significant. Data presented graphically in figures are shown as means ± standard deviations.

SUPPLEMENTARY MATERIAL

Supplementary Material is available at *HMG* online.

ACKNOWLEDGEMENTS

We thank Dr Leslie T. Webster Jr (CWRU) for valuable comments about the manuscript. We thank Dr Akiko Maeda, Neil Molyneaux, Simone Edelheit and Milena Rajak (CWRU) for technical assistance.

Conflict of Interest statement. None declared.

FUNDING

This work was supported by National Institutes of Health grants from the National Eye Institute (EY008061, EY019478, EY022606, EY022326, K08EY019880, P30 EY11373) and the Research to Prevent Blindness Foundation, Foundation Fighting Blindness, Fight for Sight and the Ohio Lions Eye Research Foundation. D.M. was supported in part by the National Institutes of Health CWRU Medical Scientist Training Program Grant (T32GM007250) and the Visual Sciences Training Grant (T32EY007157). K.P. is John H. Hord Professor of Pharmacology.

REFERENCES

1. Siegert, S., Cabuy, E., Scherf, B.G., Kohler, H., Panda, S., Le, Y.Z., Fehling, H.J., Gaidatzis, D., Stadler, M.B. and Roska, B. (2012) Transcriptional code and disease map for adult retinal cell types. *Nat. Neurosci.*, **15**, 487–495.
2. Palczewski, K. (2012) Chemistry and biology of vision. *J. Biol. Chem.*, **287**, 1612–1619.
3. Lee, R.C., Feinbaum, R.L. and Ambros, V. (1993) The C-elegans heterochronic gene Lin-4 encodes small RNAs with antisense complementarity to lin-14. *Cell*, **75**, 843–854.
4. Pasquinelli, A.E., Reinhart, B.J., Slack, F., Martindale, M.Q., Kuroda, M.I., Maller, B., Hayward, D.C., Ball, E.E., Degnan, B., Muller, P. *et al.* (2000) Conservation of the sequence and temporal expression of let-7 heterochronic regulatory RNA. *Nature*, **408**, 86–89.
5. He, L. and Hannon, G.J. (2004) Micrornas: small RNAs with a big role in gene regulation. *Nat. Rev. Genet.*, **5**, 522–531.
6. Lander, E.S., Linton, L.M., Birren, B., Nusbaum, C., Zody, M.C., Baldwin, J., Devon, K., Dewar, K., Doyle, M., FitzHugh, W. *et al.* (2001) Initial sequencing and analysis of the human genome. *Nature*, **409**, 860–921.
7. Venter, J.C., Adams, M.D., Myers, E.W., Li, P.W., Mural, R.J., Sutton, G.G., Smith, H.O., Yandell, M., Evans, C.A., Holt, R.A. *et al.* (2001) The sequence of the human genome. *Science*, **291**, 1304–1351.
8. Waterston, R.H., Lindblad-Toh, K., Birney, E., Rogers, J., Abril, J.F., Agarwal, P., Agarwala, R., Ainscough, R., Alexandersson, M., An, P. *et al.* (2002) Initial sequencing and comparative analysis of the mouse genome. *Nature*, **420**, 520–562.
9. Mercer, T.R., Dinger, M.E. and Mattick, J.S. (2009) Long non-coding RNAs: insights into functions. *Nat. Rev. Genet.*, **10**, 155–159.
10. Moran, V.A., Perera, R.J. and Khalil, A.M. (2012) Emerging functional and mechanistic paradigms of mammalian long non-coding RNAs. *Nucleic Acids Res.*, **40**, 6391–6400.
11. Cabili, M.N., Trapnell, C., Goff, L., Koziol, M., Tazon-Vega, B., Regev, A. and Rinn, J.L. (2011) Integrative annotation of human large intergenic noncoding RNAs reveals global properties and specific subclasses. *Gene. Dev.*, **25**, 1915–1927.
12. Guttman, M., Amit, I., Garber, M., French, C., Lin, M.F., Feldser, D., Huarte, M., Zuk, O., Carey, B.W., Cassady, J.P. *et al.* (2009) Chromatin signature reveals over a thousand highly conserved large non-coding RNAs in mammals. *Nature*, **458**, 223–227.
13. Khalil, A.M., Guttman, M., Huarte, M., Garber, M., Raj, A., Morales, D.R., Thomas, K., Presser, A., Bernstein, B.E., van Oudenaarden, A. *et al.* (2009) Many human large intergenic noncoding RNAs associate with chromatin-modifying complexes and affect gene expression. *Proc. Natl Acad. Sci. USA*, **106**, 11667–11672.
14. Rinn, J.L., Kertesz, M., Wang, J.K., Squazzo, S.L., Xu, X., Brugmann, S.A., Goodnough, L.H., Helms, J.A., Farnham, P.J., Segal, E. *et al.* (2007) Functional demarcation of active and silent chromatin domains in human HOX loci by noncoding RNAs. *Cell*, **129**, 1311–1323.
15. Guttman, M., Donaghey, J., Carey, B.W., Garber, M., Grenier, J.K., Munson, G., Young, G., Lucas, A.B., Ach, R., Bruhn, L. *et al.* (2011) lincRNAs act in the circuitry controlling pluripotency and differentiation. *Nature*, **477**, 295–300.
16. Ponjavic, J., Oliver, P.L., Lunter, G. and Ponting, C.P. (2009) Genomic and transcriptional co-localization of protein-coding and long non-coding RNA pairs in the developing brain. *PLoS Genet.*, **5**, e1000617.
17. Mercer, T.R., Dinger, M.E., Sunkin, S.M., Mehler, M.F. and Mattick, J.S. (2008) Specific expression of long noncoding RNAs in the mouse brain. *Proc. Natl Acad. Sci. USA*, **105**, 716–721.
18. Kapranov, P., Cheng, J., Dike, S., Nix, D.A., Duttagupta, R., Willingham, A.T., Stadler, P.F., Hertel, J., Hackermuller, J., Hofacker, I.L. *et al.* (2007) RNA maps reveal new RNA classes and a possible function for pervasive transcription. *Science*, **316**, 1484–1488.
19. Martin, L. and Chang, H.Y. (2012) Uncovering the role of genomic 'dark matter' in human disease. *J. Clin. Invest.*, **122**, 1589–1595.
20. Maass, P.G., Rump, A., Schultz, H., Stricker, S., Schulze, L., Platzer, K., Aydin, A., Tinschert, S., Goldring, M.B., Luft, F.C. *et al.* (2012) A misplaced lncRNA causes bracydactyly in humans. *J. Clin. Invest.*, **122**, 3990–4002.
21. Kumar, V., Westra, H.J., Karjalainen, J., Zhernakova, D.V., Esko, T., Hrdlickova, B., Almeida, R., Zhernakova, A., Reinmaa, E., Vosa, U. *et al.* (2013) Human disease-associated genetic variation impacts large intergenic non-coding RNA expression. *PLoS Genet.*, **9**, e1003201.
22. Talkowski, M.E., Maussion, G., Crapper, L., Rosemfeld, J.A., Blumenthal, I., Hanscom, C., Chiang, C., Lindgren, A., Pereira, S., Ruderfer, D. *et al.* (2012) Disruption of large intergenic noncoding RNA in subjects with neurodevelopmental disabilities. *Am. J. Hum. Genet.*, **91**, 1128–1134.
23. Guttman, M., Garber, M., Levin, J.Z., Donaghey, J., Robinson, J., Adiconis, X., Fan, L., Koziol, M.J., Gnirke, A., Nusbaum, C. *et al.* (2010) Ab initio reconstruction of cell type-specific transcriptomes in mouse reveals the conserved multi-exonic structure of lincRNAs. *Nat. Biotechnol.*, **28**, 503–510.
24. Ulitsky, I., Shkumatava, A., Jan, C.H., Sive, H. and Bartel, D.P. (2011) Conserved function of lincRNAs in vertebrate embryonic development despite rapid sequence evolution. *Cell*, **147**, 1537–1550.
25. Young, R.S., Marques, A.C., Tibbit, C., Haerty, W., Bassett, A.R., Liu, J.L. and Ponting, C.P. (2012) Identification and properties of 1,119 candidate lincRNA loci in the Drosophila melanogaster Genome. *Genome Biol. Evol.*, **4**, 427–442.
26. Chakraborty, D., Kappei, D., Theis, M., Nitzsche, A., Ding, L., Paszkowski-Rogacz, M., Surendranath, V., Berger, N., Schulz, H., Saar, K. *et al.* (2012) Combined RNAi and localization for functionally dissecting long noncoding RNAs. *Nat. Methods*, **9**, 360–362.
27. Guo, X., Gao, L., Liao, Q., Xiao, H., Ma, X., Yang, X., Luo, H., Zhao, G., Bu, D., Jiao, F. *et al.* (2013) Long non-coding RNAs function annotation: a global prediction method based on bi-colored networks. *Nucleic Acids Res.*, **41**, e35
28. Liao, Q., Liu, C., Yuan, X., Kang, S., Miao, R., Xiao, H., Zhao, G., Luo, H., Bu, D., Zhao, H. *et al.* (2011) Large-scale prediction of long non-coding RNA functions in a coding-non-coding gene co-expression network. *Nucleic Acids Res.*, **39**, 3864–3878.
29. Washietl, S., Hofacker, I.L., Lukasser, M., Huttenhofer, A. and Stadler, P.F. (2005) Mapping of conserved RNA secondary structures predicts thousands of functional noncoding RNAs in the human genome. *Nat. Biotechnol.*, **23**, 1383–1390.
30. Coon, S.L., Munson, P.J., Cherukuri, P.F., Sugden, D., Rath, M.F., Moller, M., Clokie, S.J.H., Fu, C., Olanich, M.E., Rangel, Z. *et al.* (2012) Circadian changes in long noncoding RNAs in the pineal gland. *Proc. Natl Acad. Sci. USA*, **109**, 13319–13324.
31. Meola, N., Pizzo, M., Alfano, G., Surace, E.M. and Banfi, S. (2012) The long noncoding RNA Vax2os1 controls the cell cycle progression of photoreceptor progenitors in the mouse retina. *RNA*, **18**, 111–123.
32. Rapicavoli, N.A., Poth, E.M. and Blackshaw, S. (2010) The long noncoding RNA RNCR2 directs mouse retinal cell specification. *BMC Dev. Biol.*, **10**, 49.

33. Rapicavoli, N.A., Poth, E.M., Zhu, H. and Blackshaw, S. (2011) The long noncoding RNA Six3OS acts in trans to regulate retinal development by modulating Six3 activity. *Neural Dev.*, **6**, 32.
34. Sone, M., Hayashi, T., Tarui, H., Agata, K., Takeichi, M. and Nakagawa, S. (2007) The mRNA-like noncoding RNA Gomafu constitutes a novel nuclear domain in a subset of neurons. *J. Cell Sci.*, **120**, 2498–2506.
35. Young, T.L., Matsuda, T. and Cepko, C.L. (2005) The noncoding RNA taurine upregulated gene 1 is required for differentiation of the murine retina. *Curr. Biol.*, **15**, 501–512.
36. Blackshaw, S., Harpavat, S., Trimarchi, J., Cai, L., Huang, H.Y., Kuo, W.P., Weber, G., Lee, K., Fraioli, R.E., Cho, S.H. *et al.* (2004) Genomic analysis of mouse retinal development. *PLoS Biol.*, **2**, 1411–1431.
37. Mustafi, D., Maeda, T., Kohno, H., Nadeau, J.H. and Palczewski, K. (2012) Inflammatory priming predisposes to age-related retinal degeneration in mice. *J. Clin. Invest.*, **122**, 2989–3001.
38. Mustafi, D., Kevany, B.M., Genoud, C., Okano, K., Cideciyan, A.V., Sumaroka, A., Roman, A.J., Jacobson, S.G., Engel, A., Adams, M.D. *et al.* (2011) Defective photoreceptor phagocytosis in a mouse model of enhanced S-cone syndrome causes progressive retinal degeneration. *FASEB J.*, **25**, 3157–3176.
39. Mortazavi, A., Williams, B.A., McCue, K., Schaeffer, L. and Wold, B. (2008) Mapping and quantifying mammalian transcriptomes by RNA-Seq. *Nat. Methods*, **5**, 621–628.
40. Curcio, C.A., Sloan, K.R., Kalina, R.E. and Hendrickson, A.E. (1990) Human photoreceptor topography. *J. Comp. Neurol.*, **292**, 497–523.
41. Provis, J.M., Penfold, P.L., Cornish, E.E., Sandercoe, T.M. and Madigan, M.C. (2005) Anatomy and development of the macula: specialisation and the vulnerability to macular degeneration. *Clin. Exp. Optom.*, **88**, 269–281.
42. Zhu, Q.B., Sun, W.Y., Okano, K., Chen, Y., Zhang, N., Maeda, T. and Palczewski, K. (2011) Sponge transgenic mouse model reveals important roles for the MicroRNA-183 (miR-183)/96/182 cluster in postmitotic photoreceptors of the retina. *J. Biol. Chem.*, **286**, 31749–31760.
43. Soucy, E., Wang, Y.S., Nirenberg, S., Nathans, J. and Meister, M. (1998) A novel signaling pathway from rod photoreceptors to ganglion cells in mammalian retina. *Neuron*, **21**, 481–493.
44. Mears, A.J., Kondo, M., Swain, P.K., Takada, Y., Bush, R.A., Saunders, T.L., Sieving, P.A. and Swaroop, A. (2001) Nrl is required for rod photoreceptor development. *Nat. Genet.*, **29**, 447–452.
45. Sakami, S., Maeda, T., Bereta, G., Okano, K., Golczak, M., Sumaroka, A., Roman, A.J., Cideciyan, A.V., Jacobson, S.G. and Palczewski, K. (2011) Probing mechanisms of photoreceptor degeneration in a new mouse model of the common form of autosomal dominant retinitis pigmentosa due to P23H opsin mutations. *J. Biol. Chem.*, **286**, 10551–10567.
46. Sun, H. and Nathans, J. (1997) Stargardt's ABCR is localized to the disc membrane of retinal rod outer segments. *Nat. Genet.*, **17**, 15–16.
47. Lerner, L.E., Peng, G.H., Gribanova, Y.E., Chen, S.M. and Farber, D.B. (2005) Sp4 is expressed in retinal neurons, activates transcription of photoreceptor-specific genes, and synergizes with Crx. *J. Biol. Chem.*, **280**, 20642–20650.
48. Chau, K.Y., Munshi, N., Keane-Myers, A., Cheung-Chau, K.W., Tai, A.K.F., Manfioletti, G., Dorey, C.K., Thanos, D., Zack, D.J. and Ono, S.J. (2000) The architectural transcription factor high mobility group I(Y) participates in photoreceptor-specific gene expression. *J. Neurosci.*, **20**, 7317–7324.
49. Ruan, G.X., Zhang, D.Q., Zhou, T.R., Yamazaki, S. and McMahon, D.G. (2006) Circadian organization of the mammalian retina. *Proc. Natl Acad. Sci. USA*, **103**, 9703–9708.
50. Rath, M.F., Bailey, M.J., Kim, J.S., Coon, S.L., Klein, D.C. and Moller, M. (2009) Developmental and daily expression of the Pax4 and Pax6 homeobox genes in the rat retina: localization of Pax4 in photoreceptor cells. *J. Neurochem.*, **108**, 285–294.
51. Li, T., Lu, Z.Y. and Lu, L. (2004) Regulation of eye development by transcription control of CCCTC binding factor (CTCF). *J. Biol. Chem.*, **279**, 27575–27583.
52. Canto-Soler, M.V., Huang, H., Romero, M.S. and Adler, R. (2008) Transcription factors CTCF and Pax6 are segregated to different cell types during retinal cell differentiation. *Dev. Dynam.*, **237**, 758–767.
53. Sopher, B.L., Ladd, P.D., Pineda, V.V., Libby, R.T., Sunkin, S.M., Hurley, J.B., Thienes, C.P., Gaasterland, T., Filippova, G.N. and La Spada, A.R. (2011) CTCF regulates ataxin-7 expression through promotion of a convergently transcribed, antisense noncoding RNA. *Neuron*, **70**, 1071–1084.
54. Ponting, C.P., Oliver, P.L. and Reik, W. (2009) Evolution and functions of long noncoding RNAs. *Cell*, **136**, 629–641.
55. Taft, R.J., Pang, K.C., Mercer, T.R., Dinger, M. and Mattick, J.S. (2010) Non-coding RNAs: regulators of disease. *J. Pathol.*, **220**, 126–139.
56. Kutter, C., Watt, S., Stefflova, K., Wilson, M.D., Goncalves, A., Ponting, C.P., Odom, D.T. and Marques, A.C. (2012) Rapid turnover of long noncoding RNAs and the evolution of gene expression. *PLoS Genet.*, **8**, e1002841.
57. Chodroff, R.A., Goodstadt, L., Sirey, T.M., Oliver, P.L., Davies, K.E., Green, E.D., Molnar, Z. and Ponting, C.P. (2010) Long noncoding RNA genes: conservation of sequence and brain expression among diverse amniotes. *Genome Biol.*, **11**, R72.
58. Quazi, F., Lenevich, S. and Molday, R.S. (2012) ABCA4 is an N-retinylidene-phosphatidylethanolamine and phosphatidylethanolamine importer. *Nat. Commun.*, **3**, 1–9.
59. Allikmets, R., Singh, N., Sun, H., Shroyer, N.E., Hutchinson, A., Chidambaram, A., Gerrard, B., Baird, L., Stauffer, D., Peiffer, A. *et al.* (1997) A photoreceptor cell-specific ATP-binding transporter gene (ABCR) is mutated in recessive Stargardt macular dystrophy. *Nat. Genet.*, **15**, 236–246.
60. Cremers, F.P.M., van De Pol, D.J.R., van Driel, M., den Hollander, A.I., van Haren, F.J.J., Knoers, N.V.A.M., Tijmes, N., Bergen, A.A.B., Rohrschneider, K., Blankenagel, A. *et al.* (1998) Autosomal recessive retinitis pigmentosa and cone-rod dystrophy caused by splice site mutations in the Stargardt's disease gene ABCR. *Hum. Mol. Genet.*, **7**, 355–362.
61. Hoppe, G., Rayborn, M.E. and Sears, J.E. (2007) Diurnal rhythm of the chromatin protein Hmgb1 in rat photoreceptors is under circadian regulation. *J. Comp. Neurol.*, **501**, 219–230.
62. Gehring, W.J. (1996) The master control gene for morphogenesis and evolution of the eye. *Genes Cells*, **1**, 11–15.
63. Reichman, S., Kalathur, R.K., Lambard, S., Ait-Ali, N., Yang, Y., Lardenois, A., Ripp, R., Poch, O., Zack, D.J., Sahel, J.A. *et al.* (2010) The homeobox gene CHX10/VSX2 regulates RdCVF promoter activity in the inner retina. *Hum. Mol. Genet.*, **19**, 250–261.
64. Leveillard, T., Mohand-Said, S., Lorentz, O., Hicks, D., Fintz, A.C., Clerin, E., Simonutti, M., Forster, V., Cavusoglu, N., Chalmel, F. *et al.* (2004) Identification and characterization of rod-derived cone viability factor. *Nat. Genet.*, **36**, 755–759.
65. Yang, Y., Mohand-Said, S., Danan, A., Simonutti, M., Fontaine, V., Clerin, E., Picaud, S., Leveillard, T. and Sahel, J.A. (2009) Functional cone rescue by RdCVF protein in a dominant model of retinitis pigmentosa. *Mol. Ther.*, **17**, 787–795.
66. Yanicostas, C., Barbieri, E., Hibi, M., Brice, A., Stevanin, G. and Soussi-Yanicostas, N. (2012) Requirement for zebrafish ataxin-7 in differentiation of photoreceptors and cerebellar neurons. *PLoS ONE*, **7**, e50705.
67. Helmlinger, D., Hardy, S., Abou-Sleymane, G., Eberlin, A., Bowman, A.B., Gansmuller, A., Picaud, S., Zoghbi, H.Y., Trottier, Y., Tora, L. *et al.* (2006) Glutamine-expanded ataxin-7 alters TFTC/STAGA recruitment and chromatin structure leading to photoreceptor dysfunction. *PLoS Biol.*, **4**, e67.
68. Palhan, V.B., Chen, S., Peng, G.H., Tjernberg, A., Gamper, A.M., Fan, Y., Chait, B.T., La Spada, A.R. and Roeder, R.G. (2005) Polyglutamine-expanded ataxin-7 inhibits STAGA histone acetyltransferase activity to produce retinal degeneration. *Proc. Natl Acad. Sci. USA*, **102**, 8472–8477.
69. Kahle, J.J., Gulbahce, N., Shaw, C.A., Lim, J., Hill, D.E., Barabasi, A.L. and Zoghbi, H.Y. (2011) Comparison of an expanded ataxia interactome with patient medical records reveals a relationship between macular degeneration and ataxia. *Hum. Mol. Genet.*, **20**, 510–527.
70. Orom, U.A., Derrien, T., Beringer, M., Gumireddy, K., Gardini, A., Bussotti, G., Lai, F., Zytnicki, M., Notredame, C., Huang, Q.H. *et al.* (2010) Long noncoding RNAs with enhancer-like function in human cells. *Cell*, **143**, 46–58.
71. Djebali, S., Davis, C.A., Merkel, A., Dobin, A., Lassmann, T., Mortazavi, A., Tanzer, A., Lagarde, J., Lin, W., Schlesinger, F. *et al.* (2012) Landscape of transcription in human cells. *Nature*, **489**, 101–108.
72. Burd, C.E., Jeck, W.R., Liu, Y., Sanoff, H.K., Wang, Z. and Sharpless, N.E. (2010) Expression of linear and novel circular forms of an INK4/ARF-associated non-coding RNA correlates with atherosclerosis risk. *PLoS Genet.*, **6**, e1001233.

73. Gupta, R.A., Shah, N., Wang, K.C., Kim, J., Horlings, H.M., Wong, D.J., Tsai, M.C., Hung, T., Argani, P., Rinn, J.L. *et al.* (2010) Long non-coding RNA HOTAIR reprograms chromatin state to promote cancer metastasis. *Nature*, **464**, 1071–1076.
74. Wheeler, T.M., Leger, A.J., Pandey, S.K., MacLeod, A.R., Nakamori, M., Cheng, S.H., Wentworth, B.M., Bennett, C.F. and Thornton, C.A. (2012) Targeting nuclear RNA for in vivo correction of myotonic dystrophy. *Nature*, **488**, 111–115.
75. Trapnell, C., Pachter, L. and Salzberg, S.L. (2009) TopHat: discovering splice junctions with RNA-Seq. *Bioinformatics*, **25**, 1105–1111.
76. Grant, C.E., Bailey, T.L. and Noble, W.S. (2011) FIMO: scanning for occurrences of a given motif. *Bioinformatics*, **27**, 1017–1018.
77. Maeda, A., Maeda, T., Imanishi, Y., Kuksa, V., Alekseev, A., Bronson, J.D., Zhang, H.B., Zhu, L., Sun, W.Y., Saperstein, D.A. *et al.* (2005) Role of photoreceptor-specific retinol dehydrogenase in the retinoid cycle in vivo. *J. Biol. Chem.*, **280**, 18822–18832.